Cureus
Part of SPRINGER NATURE

Open Access Original Article

Computed Tomography-Based Morphology and Morphometry of the Foramen Magnum and Their Associations With Sex and Age: A Cross-Sectional Study

Review began 10/21/2026
Review ended 10/30/2026
Published 11/01/2026

© **Copyright** 2026
Kumar et al. This is an open access article distributed under the terms of the Creative Commons Attribution License CC-BY 4.0., which permits unrestricted use, distribution, and reproduction in any medium, provided the original author and source are credited.

DOI: 10.7759/cureus.118965

Bhavesh Kumar [1], Kantilal M. Parmar [1], Shivani Chawla [2]

1. Department of Anatomy, Parul Institute of Medical Sciences and Research, Vadodara, IND 2. Department of Anatomy, Pandit Neki Ram Sharma Government Medical College, Bhiwani, IND

Corresponding author: Bhavesh Kumar, dr.bhaveshkumar.02@gmail.com

Abstract

Background

Foramen magnum (FM) morphology and dimensions matter in craniovertebral junction surgery and forensic sex estimation; however, computed tomography (CT) data from Gujarat, western India, are scarce. The primary aim was to compare FM diameters between men and women; secondary aims were to describe FM shape and examine the associations of shape and FM measurements with sex and age.

Materials and methods

This cross-sectional CT study analyzed 100 adults (50 men and 50 women) aged 18-55 years who were recruited using sex-stratified quota sampling. FM shape was classified into eight categories, and anteroposterior (AP) and transverse (TD) diameters were measured; estimated area and FM index were derived. Sex- and age-related associations were analyzed using Welch t-tests with 95% confidence intervals (CIs) and Holm correction, sex-adjusted regression of continuous age, and Fisher-Freeman-Halton exact tests. Intraobserver and interobserver reliability were assessed using 20 participant-linked repeat-reading records (10 per sex).

Results

Hexagonal (24%), oval (19%), and irregular (15%) were the most common FM outlines. No statistically significant shape association was detected between sex (exact $p = 0.509$) and age group ($p = 0.162$). Men had larger AP diameters (mean difference: 2.04 mm, 95% CI: 0.93-3.14), TD (2.11 mm, 1.18-3.04), and estimated area (103.3 mm^2, 60.9-145.8; Holm-adjusted $p < 0.001$ for each). The FM index was not significantly different ($p = 0.409$). No statistically significant age effect was detected. In 20 linked scans, intraobserver and interobserver shape agreement was 90% ($\kappa = 0.882$) and 80% ($\kappa = 0.763$), respectively; absolute-agreement intraclass correlation coefficients (ICCs) for the diameters ranged from 0.989 to 0.998. The originally unusual TD > AP measurements for participant 27 were similar on both repeats, and all readings were labeled as FM pentagonal.

Conclusions

In this single-center sample, FM linear dimensions and estimated area were greater in men. Shape, index, and age comparisons were not significant, although modest associations cannot be excluded. Repeat readings showed strong within-sample observer agreement, and independent Digital Imaging and Communications in Medicine (DICOM) review confirmed the unusual wider-than-long FM without an identified osseous abnormality. The native axial measurement plane remains a limitation. The descriptive findings do not establish a validated forensic sex-estimation method.

Categories: Otolaryngology, Anatomy
Keywords: computed tomography, craniovertebral junction, foramen magnum, foramen magnum index, forensic anthropology, morphometry, radinsky's formula, sexual dimorphism

Introduction

The foramen magnum (FM) is the largest opening in the occipital bone and connects the posterior cranial fossa with the vertebral canal. It transmits the medulla oblongata and its meninges, the vertebral arteries, the anterior and posterior spinal arteries, and the spinal roots of the accessory nerves. The tectorial membrane passes through it to the clivus, the apical ligament of the dens attaches to its anterior margin, and the alar ligaments attach to the adjacent medial surfaces of the occipital condyles [1,2]. Bordered by the occipital condyles and located close to the hypoglossal canals and jugular foramina, the FM is a key landmark at the craniovertebral junction [1,2]. Its configuration varies among individuals; therefore,

knowledge of its normal morphology and dimensions is relevant to anatomical assessment and clinical practice [3].

Surgically, the FM is accessed through far-lateral and transcondylar approaches. Its anteroposterior (AP) and transverse (TD) dimensions, together with the shape of the occipital condyles, influence the working angle available for anteriorly located lesions, such as FM meningiomas, and the extent of condylar resection that may be required. The same corridor contains the lower cranial nerves (IX-XII) and the vertebral artery, which must be protected or decompressed [1,2]. In a series of anterolateral FM meningiomas, an "ovoid" FM, defined according to that study's shape classification, was associated with more complications and a lower extent of resection [4], whereas a separate classification grouped FM meningiomas according to their topographic position relative to the neurovascular bundle rather than FM shape [5]. The oval category used in the present study was not defined in the same way as the ovoid shape in that surgical series; therefore, the two are not directly interchangeable. FM dimensions are also considered when evaluating Chiari I deformity, and narrowing of the FM may cause cervicomedullary compression in achondroplasia [6,7]. Computed tomography (CT) allows assessment of the bony margins in living individuals and provides a practical means of measuring the FM and describing its outline.

The FM is also studied in forensic anthropology because the cranial base is relatively protected and may survive when other parts of the skull are fragmented. CT studies and systematic reviews generally report larger AP and TD diameters in men; however, the size of these differences and the accuracy of sex classification vary across populations, and FM measurements are regarded as an adjunct rather than a standalone method of sex estimation [8-10]. A statistically significant difference in group means does not, by itself, establish useful individual-level classification, and classification accuracy was not an objective of the present study.

Published FM dimensions differ according to population, imaging modality, measurement conventions, and observer [3,11-14]. In India, a cone-beam CT (CBCT) study of 200 adults from coastal Karnataka measured sagittal and TD FM diameters on axial sections and reported univariate sex-classification accuracies of up to 73.5% but did not assess FM shape [11]. In Gujarat, CT-based craniometric sex estimation has been developed in a sample of 300 adults using cranial measurements and discriminant function analysis [15]. We did not perform a systematic literature search and did not identify a CT study from Gujarat that reported FM shape and dimensions together in the same adult sample. Because ethnicity and community were not recorded, the present data cannot establish whether this population differs from other Indian groups; rather, they provide locally obtained descriptive values measured using a stated protocol.

The primary objective of this study was to compare the AP and TD diameters of the FM between men and women on CT. The secondary objectives were to describe FM shape, compare the estimated FM area and FM index between the sexes, and examine the associations of FM shape and all four measurements with age, analyzed both as two groups and as a continuous variable. Comparable sex differences in FM diameters have been reported in other CT series [8,10]. Based on previous studies, we expected larger mean AP and TD diameters in men; the shape and age analyses were exploratory.

Materials And Methods

Study design, participants, and ethics

This cross-sectional observational study was conducted in the Departments of Anatomy and Radiology at Parul Institute of Medical Sciences and Research and Parul Sevashram Hospital, Vadodara, Gujarat, India, from January 2025 to February 2026. The report follows the relevant STROBE (Strengthening the Reporting of Observational Studies in Epidemiology) guidance for cross-sectional studies. Consecutive sex-specific quota sampling was used: adults aged 18-55 years undergoing clinically indicated head and neck CT were screened sequentially, and eligible participants were enrolled within each sex stratum until 50 men and 50 women were included. Of the 138 scans screened, 38 were excluded for the following reasons: craniocervical trauma or skull-base fracture (n = 14); indistinct FM cortical margins due to motion or beam-hardening artifacts (n = 12); neoplastic, infectious, or metabolic bone lesions affecting FM morphology (n = 5); prior skull-base or craniovertebral surgery (n = 4); and congenital craniovertebral anomalies (n = 3; two cases of atlanto-occipital assimilation and one of basilar invagination).

The final analytical sample comprised 100 participants (Table *1*). Among the included participants, the CT indications were headache or migraine evaluation (n = 34), sinonasal disease (n = 28), minor trauma without fracture (n = 19), suspected otological or mastoid infection (n = 11), and cervical pain or vertigo without osseous pathology (n = 8). Ethnicity or community, height, weight, and head size were not recorded. The screening register was reviewed against departmental recruitment records, confirming the 138 patients screened, the 38 exclusions and their recorded reasons, and the final sex-stratified quota sample.

Inclusion criteria	Exclusion criteria
Age 18–55 years at the time of imaging	Craniocervical trauma or fracture
Clinically indicated head and neck CT performed between January 2025 and February 2026	Prior skull-base or craniovertebral surgery
Intact FM, clearly visualized on axial images	Congenital anomaly (e.g., atlanto-occipital assimilation, basilar invagination, platybasia, condylar hypoplasia, or Chiari malformation)
Clearly delineated FM bony margins on CT	Lesion distorting the FM (e.g., neoplastic, infectious, or metabolic bone disease, including Paget disease, fibrous dysplasia, osteomalacia, or acromegaly) or indistinct margins from motion/beam-hardening artifacts

TABLE 1: Inclusion and exclusion criteria

Scans were excluded for reasons described in the text (38 of 138 screened); the final sex-balanced quota sample comprised 100 adults. Indistinct margins were those insufficiently resolved for reliable cortical landmark placement because of motion or beam-hardening artifacts.

CT: Computed tomography; FM: Foramen magnum.

The eligible age range of 18-55 years was selected to limit the potential influence of later-life osteophytosis, ligamentous calcification, and hyperostosis at the craniovertebral junction. The two age groups (18-34 years, n = 48; 35-55 years, n = 52) and the age cut-off at 35 years were specified in the ethics-approved protocol. As the cut-off has no established anatomical threshold, age was also analyzed continuously. No a priori sample size calculation was performed; enrollment followed the planned sex quotas within the study period. For 50 participants per sex, an approximate detectable-effect calculation indicates 80% power (two-sided $\alpha = 0.05$) for a standardized mean difference of about 0.57 (approximately 1.6 mm for an AP standard deviation (SD) of 2.8 mm), but the eight-category shape tests had limited power for modest associations.

The Parul University Institutional Ethics Committee for Human Research approved the protocol on December 31, 2024 (PUIECHR/PIMSR/00/081734/8207). Written informed consent was obtained from all participants. CT scans were acquired solely for clinical indications, without additional research-related radiation, and the analyses used anonymized records.

Imaging Protocol

All examinations were obtained using a 16-row Siemens SOMATOM Emotion 16 multidetector CT scanner (Siemens Healthineers, Erlangen, Germany), with 16 × 0.6-mm detector collimation, 120 kVp, effective 200 mAs with CARE Dose4D tube-current modulation, 0.8 pitch, and 1.0-s rotation time. Axial images were reconstructed at 1.0-mm thickness with a 0.5-mm reconstruction increment using the H70s sharp bone kernel. The display field of view was 220 × 220 mm with a 512 × 512 matrix (in-plane pixel size, approximately 0.43 × 0.43 mm). Patients were scanned in the supine position using a dedicated head holder, with the midsagittal plane centered, the orbitomeatal line perpendicular to the table, and the gantry tilt at 0°. Images were reviewed on the MedSynapse picture archiving and communication system (PACS) workstation (version 7.0.0.0 RC2 P6; MedSynaptic Pvt. Ltd., Pune, India) at 2× digital magnification using standardized bone-window settings (width 2,000 Hounsfield units; level 400 Hounsfield units). Native axial sections at the greatest apparent FM aperture were used; no oblique multiplanar reformatting was performed. Scanner identity and acquisition/reconstruction settings were cross-checked against the radiology department's CT protocol and acquisition records.

Morphological Assessment

The FM outline was classified on the 1.0-mm native axial section showing its widest aperture into oval, round, tetragonal, pentagonal, hexagonal, heptagonal, octagonal, or irregular types, adapted from Aljarrah et al. (Figure *1*) [12]. Polygonal types were assigned by counting four, five, six, seven, or eight distinct angular changes along the inner bony cortex; smoothly curved segments were not treated as sides. Oval denoted a smoothly rounded AP-elongated contour without discernible vertices; round denoted a near-circular contour with approximately equal diameters. Asymmetrical outlines or margins with notches, tubercles, or projections precluding the other categories were classified as irregular. The primary readings were performed by Bhavesh Kumar (Assistant Professor of Anatomy, with five years of experience in CT morphometry), who was blinded to participant identifiers, sex, and age by suppressing demographic overlays. Bhavesh Kumar and Kantilal M Parmar (Professor of Anatomy with 15 years of experience) calibrated the rubric and landmarks using 10 pilot scans before study measurements. Shape classification remains partly subjective

because apparent angles depend on the section plane and cortical display.

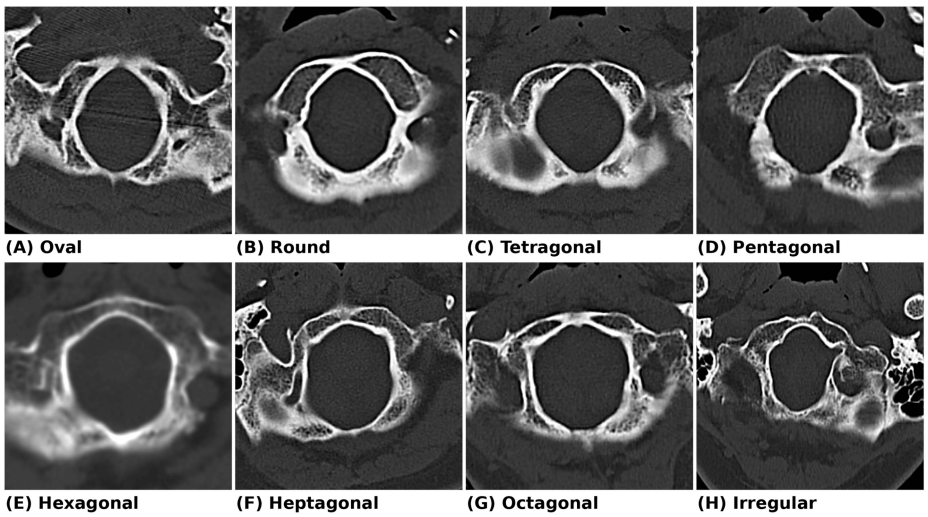


FIGURE 1: Eight CT morphological types

(A) Oval, (B) round, (C) tetragonal, (D) pentagonal, (E) hexagonal, (F) heptagonal, (G) octagonal, and (H) irregular. Polygonal types reflect the apparent number of sides; an oval is AP-elongated, a round outline is near-circular, and an irregular outline fits none of these categories. This classification is adapted from Aljarrah et al. [12].

Image credit: This is an original, previously unpublished image acquired at the authors' institution as part of the present study. It has not been reproduced or adapted from any published source; therefore, permission from a third-party copyright holder was not required.

Morphometric Assessment

The AP diameter was measured as the basion-to-opisthion distance and TD as the largest FM width perpendicular to the AP line, using workstation calipers (Figure *2*). Measurements were obtained from the native 1.0-mm axial image with the widest apparent aperture, without oblique or FM-aligned multiplanar reformats. The gantry tilt was 0°, and the head position was standardized as described above. As the FM plane is oblique, axial assessment may not coincide with the true midsagittal basion-opisthion axis and may underestimate AP length relative to anatomically aligned reconstructions. This limitation is retained despite acquisition standardization.

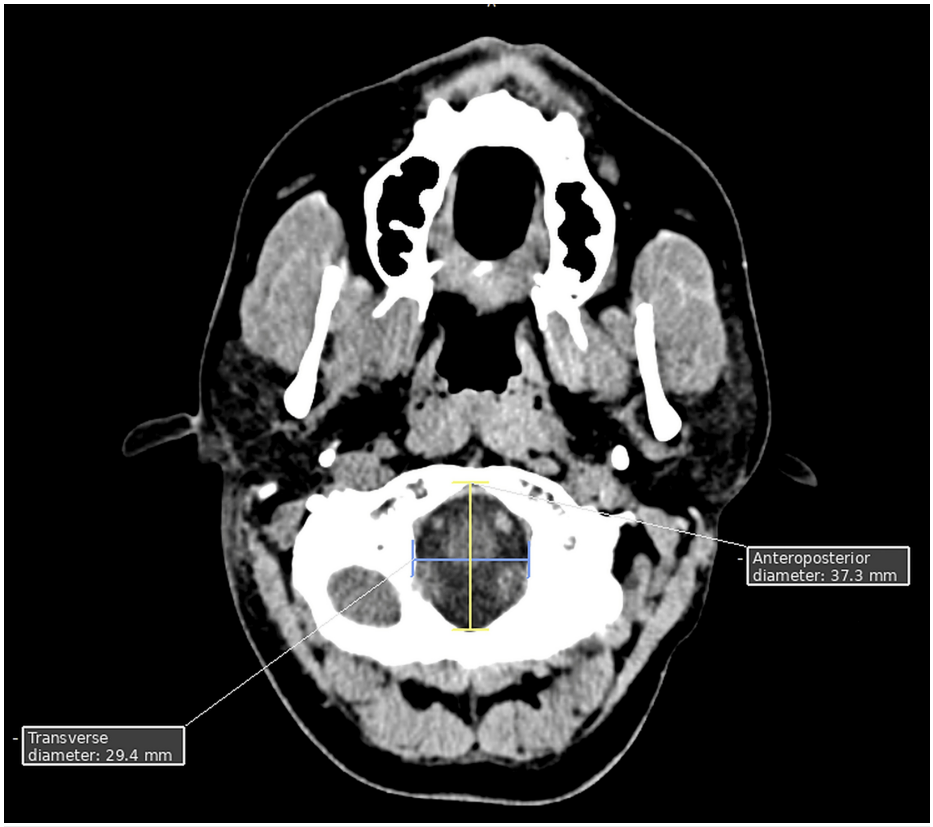


FIGURE 2: CT measurement of the foramen magnum

Axial bone-window image at the widest aperture demonstrating AP (basion to opisthion: 37.3 mm) and TD (perpendicular width: 29.4 mm).

Image credit: This is an original, previously unpublished image acquired at the authors' institution as part of the present study. It has not been reproduced or adapted from any published source; therefore, permission from a third-party copyright holder was not required.

Diameters were recorded in centimeters to two decimal places and converted to millimeters. Estimated FM area was recalculated for each participant from the original AP and TD measurements using Radinsky's formula, area = (π/4) × AP × TD [3,10]. The original master chart had used 0.785 as an approximation to π/4; the more precise factor was applied consistently in the reported analysis, which explains small differences between the chart's stored areas and the manuscript's results. The dimensionless FM index was calculated as (TD/AP) × 100 [1]. All derived values and statistical comparisons were checked against the 100 participant-level records.

Statistical analysis

Measurements from the 100-participant master chart were extracted and independently recalculated using Python (Python Software Foundation, Wilmington, DE), pandas, SciPy, and statsmodels; the study's original analysis was performed by IBM SPSS Statistics version 25 (IBM Corp., Armonk, NY). Categorical variables are presented as counts and percentages; continuous measurements as mean ± SD, median (interquartile range (IQR)), and range.

The AP and TD diameters were the primary outcomes; the estimated area and FM index were secondary, derived outcomes. Differences between men and women and between the two age groups were assessed using Welch's unequal-variance t-test for all comparisons. Preliminary tests of normality or variance homogeneity were not used to select the test. For each comparison, the mean difference with its 95% confidence interval (CI), the t statistic with Welch-Satterthwaite degrees of freedom (df), and Cohen's d (mean difference divided by the pooled SD) are reported. As four parameters were compared within each of the two comparison families (sex and age group), p-values were adjusted within each family using the Holm-Bonferroni procedure. Mann-Whitney U tests were used as distribution-free sensitivity analyses. To use the full age information, each parameter was also regressed on age (years) and sex by multiple linear regression, and an age × sex interaction was tested in a separate model. Age effects are expressed per 10 years, with 95% CIs.

Shape associations with sex and age group were tested using 8 × 2 Fisher-Freeman-Halton fixed-margin exact tests because 6/16 (37.5%) and 7/16 (43.8%) expected counts were below five, respectively. The probability-ordered exact p-values were obtained by complete enumeration of the contingency tables sharing the observed margins. The results were independently reproduced from the participant-level master chart using the analysis code supplied with the study. Asymptotic chi-square values are shown for comparison only. Cramér's V, bias-corrected V, and percentile bootstrap CIs describe the uncertain magnitude of association. Exploratory analyses regrouped shapes as curved (oval/round), polygonal (tetragonal through octagonal), and irregular; this regrouping was not prespecified. Observer agreement was assessed using the designated 20-scan subsample, with matched original, repeat, and blinded second-observer measurements: unweighted Cohen's kappa was used for the eight-category shape and two-way random-effects single-measure absolute-agreement intraclass correlation coefficient (ICC; 2,1) for AP and TD, each with 95% CIs. Bland-Altman mean differences and 95% limits of agreement (LoA) were also estimated. Observer 1 repeated the measurements after a four-week interval, while observer 2 independently assessed de-identified images without access to the original measurements or participant demographics.

A two-sided p-value of less than 0.05 was considered statistically significant. Nonsignificant results are interpreted as an absence of evidence of a difference rather than as evidence of equivalence and are accompanied by CIs. Observations lying beyond 1.5 times the IQR were identified and retained, and their influence was examined in a sensitivity analysis that excluded them.

Intraobserver and interobserver reliability were evaluated in 20 selected CT scans (10 men and 10 women). Initial, repeat, and independent second-observer measurements were linked by participant identifier; only these 20 scans contributed to the agreement estimates. The original Digital Imaging and Communications in Medicine (DICOM) series of the participant with an unusually wide FM was additionally reviewed, as described below.

Results

Participant characteristics

The 100 participants had a mean age of 35.34 ± 11.47 years (18-55 years). The respective mean ages of men and women were 35.22 ± 11.38 and 35.46 ± 11.67 years (p = 0.917); 25 men and 23 women were in age group I; 25 men and 27 women were in age group II; the distributions were similar (p = 0.841) (Table 2).

Group	n	Age, mean ± SD (years)	Age range (years)	Age group I, 18-34 years, n (%)	Age group II, 35-55 years, n (%)
Men	50	35.22 ± 11.38	18-55	25 (50%)	25 (50%)
Women	50	35.46 ± 11.67	18-53	23 (46%)	27 (54%)
Total	100	35.34 ± 11.47	18-55	48 (48%)	52 (52%)

TABLE 2: Demographic characteristics of the study participants

Percentages are calculated within each sex for the respective sex-specific rows and within the total sample for the overall row.

SD: Standard deviation.

Morphological findings

The most frequent shapes were hexagonal (n = 24, 24%), oval (n = 19, 19%), and irregular (n = 15, 15%), followed by heptagonal (n = 12, 12%), tetragonal (n = 10, 10%), octagonal (n = 8, 8%), and round (n = 7, 7%); pentagonal was least frequent (n = 5, 5%). Hexagonal was the most frequent shape in men (n = 13, 26%) and oval in women (n = 12, 24%), and tetragonal outlines were more frequent in men (n = 8, 16%) than in women (n = 2, 4%) (Table 3).

Shape	Men (n = 50), n (%)	Women (n = 50), n (%)	Total (n = 100), n (%)
Hexagonal	13 (26%)	11 (22%)	24 (24%)
Oval	7 (14%)	12 (24%)	19 (19%)
Irregular	8 (16%)	7 (14%)	15 (15%)
Heptagonal	5 (10%)	7 (14%)	12 (12%)
Tetragonal	8 (16%)	2 (4%)	10 (10%)
Octagonal	3 (6%)	5 (10%)	8 (8%)
Round	4 (8%)	3 (6%)	7 (7%)
Pentagonal	2 (4%)	3 (6%)	5 (5%)
Total	50 (100%)	50 (100%)	100 (100%)

TABLE 3: Distribution of foramen magnum shapes by sex (n = 100)

Percentages are calculated within each sex. The Fisher–Freeman–Halton exact test was the primary test (p = 0.509); the asymptotic Pearson chi-square test yielded $\chi^2 = 6.33$, df = 7, and p = 0.502. Cramér's V was 0.252. Six of the 16 expected cell counts (37.5%) were below five; therefore, the asymptotic test is presented for comparison only.

No statistically significant association between shape and sex was detected (Fisher-Freeman-Halton exact p = 0.509; $\chi^2 = 6.33$, df = 7, p = 0.502; Cramér's V = 0.25; bias-corrected V = 0.00, 95% CI = 0.00-0.43). Oval outlines were more frequent in age group I (n = 13, 27.1%) than in age group II (n = 6, 11.5%), and tetragonal outlines were less frequent (n = 2, 4.2% vs. n = 8, 15.4%), but no statistically significant association between shape and age group was detected (exact p = 0.162; $\chi^2 = 10.65$, df = 7, p = 0.155; Cramér's V = 0.33; bias-corrected V = 0.19, 95% CI = 0.00-0.49) (Table *4*). The wide CIs show that these tests were imprecise and that modest associations cannot be excluded. The corresponding two-sided fixed-margin exact p-values, independently reproduced by enumeration, were 0.509075 and 0.161685, respectively.

Shape	Age group I, 18-34 years (n = 48), n (%)	Age group II, 35-55 years (n = 52), n (%)	Total (n = 100), n (%)
Hexagonal	11 (22.9%)	13 (25.0%)	24 (24%)
Oval	13 (27.1%)	6 (11.5%)	19 (19%)
Irregular	10 (20.8%)	5 (9.6%)	15 (15%)
Heptagonal	5 (10.4%)	7 (13.5%)	12 (12%)
Tetragonal	2 (4.2%)	8 (15.4%)	10 (10%)
Octagonal	3 (6.2%)	5 (9.6%)	8 (8%)
Round	3 (6.2%)	4 (7.7%)	7 (7%)
Pentagonal	1 (2.1%)	4 (7.7%)	5 (5%)
Total	48 (100%)	52 (100%)	100 (100%)

TABLE 4: Distribution of foramen magnum shapes by age group (n = 100)

Percentages are calculated within age groups. The Fisher–Freeman–Halton exact test yielded p = 0.162, and Cramér's V was 0.326. Seven of the 16 expected cell counts were below five.

In the exploratory three-category analysis, curved, polygonal, and irregular outlines did not differ significantly by sex (men: n = 11, 22%; n = 31, 62%; and n = 8, 16%; women: n = 15, 30%; n = 28, 56%; and n = 7, 14%; exact p = 0.667; $\chi^2 = 0.83$, df = 2; V = 0.09). Polygonal outlines were more frequent in age group II (n = 37, 71.2%) than in age group I (n = 22, 45.8%), with curved (n = 16, 33.3% vs. n = 10, 19.2%) and irregular outlines (n = 10, 20.8% vs. n = 5, 9.6%) correspondingly less frequent (exact p = 0.038; $\chi^2 = 6.72$, df = 2; V = 0.26). Because this analysis was not prespecified and was not adjusted for multiple testing, it is hypothesis-

generating only. The number of sides of polygonal outlines did not differ significantly by sex (median 6 in both; p = 0.087) or by age group (median 6 in both; p = 0.326).

Morphometric findings

Descriptive statistics are given in Table 5 and group comparisons in Table 6. Men had a larger AP diameter than women (mean difference = 2.04 mm, 95% CI = 0.93-3.14; Welch t = 3.65, df = 97.2; Cohen's d = 0.73), a larger TD (2.11 mm, 1.18-3.04; t = 4.51, df = 98.0; d = 0.90), and a larger estimated area (103.3 mm², 60.9-145.8; t = 4.83, df = 96.0; d = 0.97); all three differences remained significant after Holm adjustment (all adjusted p < 0.001). These differences corresponded to 6.0%, 7.4%, and 13.4% of the female means. The FM index did not differ significantly between the sexes (difference = 1.22, 95% CI = −1.70 to 4.13; p = 0.409; d = 0.17).

Parameter	Group	n	Mean ± SD	Median (IQR)	Range
Anteroposterior diameter (mm)	Men	50	36.11 ± 2.66	36.80 (34.23–37.77)	30.60–41.30
	Women	50	34.07 ± 2.91	33.90 (32.10–36.27)	28.20–40.40
	Age group I (18–34 years)	48	35.03 ± 2.91	35.00 (33.05–37.32)	29.30–40.40
	Age group II (35–55 years)	52	35.14 ± 3.03	35.35 (32.80–37.12)	28.20–41.30
Transverse diameter (mm)	Men	50	30.78 ± 2.33	30.55 (28.90–32.58)	26.50–36.00
	Women	50	28.67 ± 2.35	28.70 (27.32–30.15)	23.50–34.10
	Age group I (18–34 years)	48	29.50 ± 2.09	29.35 (28.30–30.62)	24.00–34.10
	Age group II (35–55 years)	52	29.93 ± 2.93	29.55 (28.10–31.90)	23.50–36.00
Area (mm²)	Men	50	873.75 ± 99.00	868.19 (811.96–937.25)	651.45–1103.44
	Women	50	770.41 ± 114.30	751.07 (695.18–844.41)	548.17–1023.08
	Age group I (18–34 years)	48	814.69 ± 112.08	826.59 (733.01–889.45)	569.26–1041.42
	Age group II (35–55 years)	52	828.91 ± 124.61	844.22 (737.52–911.49)	548.17–1103.44
Foramen magnum index	Men	50	85.63 ± 8.26	86.13 (79.84–90.58)	69.52–110.77
	Women	50	84.41 ± 6.29	84.59 (80.21–89.84)	67.96–98.29
	Age group I (18–34 years)	48	84.49 ± 5.62	84.95 (80.62–88.39)	73.04–98.29
	Age group II (35–55 years)	52	85.52 ± 8.64	86.21 (79.70–90.82)	67.96–110.77

TABLE 5: Descriptive statistics of foramen magnum parameters by sex and age group

Range values represent the minimum and maximum. Estimated FM area was calculated as (π/4) × AP × TD (mm²) using each participant's original diameter measurements; the FM index was calculated as (TD/AP) × 100. The original chart stored area values using 0.785 as an approximation of π/4. Only group summaries are presented; whole-sample values are not repeated.

SD: Standard deviation; IQR: Interquartile range.

Comparison/parameter	Mean difference (95% CI)	Welch t (df)	p	Holm p	Cohen's d
Sex: AP diameter (mm)	2.04 (0.93 to 3.14)	3.65 (97.2)	<0.001	<0.001	0.73
Sex: Transverse diameter (mm)	2.11 (1.18 to 3.04)	4.51 (98.0)	<0.001	<0.001	0.9
Sex: Estimated area (mm²)	103.3 (60.9 to 145.8)	4.83 (96.0)	<0.001	<0.001	0.97
Sex: Foramen magnum index	1.22 (−1.70 to 4.13)	0.83 (91.5)	0.409	0.409	0.17
Age: AP diameter (mm)	0.11 (−1.07 to 1.29)	0.19 (97.9)	0.85	1	0.04
Age: Transverse diameter (mm)	0.43 (−0.57 to 1.43)	0.85 (92.2)	0.397	1	0.17
Age: Estimated area (mm²)	14.2 (−32.8 to 61.2)	0.60 (97.9)	0.549	1	0.12
Age: Foramen magnum index	1.03 (−1.84 to 3.91)	0.71 (88.4)	0.478	1	0.14

TABLE 6: Comparison of foramen magnum parameters between sexes and age groups

Sex comparisons are expressed as men minus women; age-group comparisons are expressed as group II (35–55 years) minus group I (18–34 years). Mann–Whitney U sensitivity analyses yielded the same conclusions. Nonsignificant results do not establish equivalence.

CI: Confidence interval; df: Welch–Satterthwaite degrees of freedom; Holm p: Holm–Bonferroni adjusted within each family of four comparisons; Cohen's d: Mean difference divided by the pooled standard deviation.

None of the four parameters differed significantly between the age groups (Welch p = 0.397-0.850; all Holm-adjusted p = 1.000). The 95% CIs for the differences (age group II minus age group I) were −1.07 to 1.29 mm for the AP diameter, −0.57 to 1.43 mm for TD, −32.8 to 61.2 mm² for area, and −1.84 to 3.91 for the FM index; they therefore do not exclude differences of up to about 1.3-1.4 mm, roughly two-thirds of the observed sex difference. When age was analyzed as a continuous variable with adjustment for sex, no parameter was significantly associated with age (Table 7); the estimated change per 10 years was 0.06 mm (95% CI = −0.43 to 0.55) for the AP diameter and 0.16 mm (−0.25 to 0.56) for TD, and no age × sex interaction was statistically significant (p = 0.097-0.921). Mann-Whitney U tests gave the same conclusions for all comparisons.

Parameter	Change per 10 years, adjusted for sex (95% CI)	p	Age × sex interaction (p)	Pearson r with age (p)
Anteroposterior diameter (mm)	0.06 (−0.43 to 0.55)	0.809	0.097	0.02 (0.847)
Transverse diameter (mm)	0.16 (−0.25 to 0.56)	0.449	0.921	0.07 (0.516)
Area (mm²)	5.8 (−12.8 to 24.5)	0.537	0.376	0.05 (0.609)
Foramen magnum index	0.33 (−0.95 to 1.61)	0.613	0.142	0.05 (0.618)

TABLE 7: Association of foramen magnum parameters with age analyzed as a continuous variable

Multiple linear regression was performed for each parameter using age (years) and sex as predictors (n = 100), with the age × sex interaction tested in a separate model. Regression coefficients, associated CIs, p-values, and Pearson correlation coefficients were independently reproduced from the participant-level master chart.

CI: Confidence interval.

Two observations lay beyond the 1.5 × IQR fences: a TD of 24.0 mm in a 31-year-old woman (participant 70) and an FM index of 110.77 in a 36-year-old man (participant 27; original AP, 32.5 mm; TD, 36.0 mm; estimated area, 918.92 mm²). In the linked records, participant 27 had repeat AP/TD measurements of 32.6/35.9 mm (observer 1) and 32.4/35.8 mm (observer 2), and all three readings classified the shape as pentagonal. The original 1.0-mm bone-window DICOM series for participant 27 was independently reviewed by a second observer. Repeat measurements on the source images confirmed the wider-than-long configuration, without evidence of AP/TD transposition or caliper-placement error. Multislice assessment of the occipital bone, clivus, occipital condyles, and atlas showed intact bony margins, without basilar invagination, platybasia, atlanto-occipital assimilation, condylar hypoplasia, fracture, or destructive or proliferative osseous disease. TD exceeded AP in two participants (IDs 27 and 30, with indices of 110.77 and

100.90, respectively) and equaled AP in one participant (ID 47). The recorded diameters were retained. Excluding the two IQR-defined outliers (n = 98) did not alter the conclusions: sex differences in AP, TD, and estimated area remained significant (all $p < 0.001$), whereas age-group comparisons remained nonsignificant ($p = 0.691$-0.917).

Measurement reproducibility in the linked subsample

Twenty CT scans (10 men and 10 women) were assessed for reproducibility using repeat measurements by observer 1 and independent, blinded measurements by observer 2. Shape agreement was 18/20 (90%; unweighted $\kappa = 0.882$, 95% CI = 0.727-1.000) within observer 1 and 16/20 (80%; $\kappa = 0.763$, 95% CI = 0.559-0.966) between observers. Agreement of the AP and TD diameters was high (intraobserver ICCs = 0.996 and 0.998; interobserver ICCs = 0.989 and 0.993; Table *8*). Kappa CIs are asymptotic Wald intervals with the upper limit truncated at the mathematical maximum of 1.000; the estimates are imprecise because n = 20. Participant 27 retained a pentagonal classification in all three readings.

Measure	Comparison	Agreement/reliability (95% CI)	Mean difference (95% LoA), mm
Shape (8 categories)	Intraobserver	18/20 (90%); κ = 0.882 (0.727–1.000)	—
Shape (8 categories)	Interobserver	16/20 (80%); κ = 0.763 (0.559–0.966)	—
AP diameter	Intraobserver	ICC = 0.996 (0.991–0.999)	+0.015 (−0.522 to +0.552)
TD diameter	Intraobserver	ICC = 0.998 (0.994–0.999)	−0.015 (−0.419 to +0.389)
AP diameter	Interobserver	ICC = 0.989 (0.974–0.996)	+0.045 (−0.849 to +0.939)
TD diameter	Interobserver	ICC = 0.993 (0.981–0.997)	−0.025 (−0.741 to +0.691)

TABLE 8: Intra- and interobserver reliability in the linked 20-participant subsample

AP: Anteroposterior; TD: Transverse; SD: Standard deviation; ICC: Two-way random-effects, single-measure, absolute-agreement intraclass correlation coefficient ICC (2,1); κ: Unweighted Cohen's kappa; CI: Confidence interval; LoA: Bland–Altman limits of agreement (mean paired difference ± 1.96 SD).

Intraobserver differences were calculated as the initial reading minus the repeat reading; interobserver differences were calculated as the initial reading by observer 1 minus the blinded reading by observer 2. Kappa CIs were calculated using asymptotic standard errors, bounded above at 1.000. Reliability was evaluated in the selected 20-scan subsample.

Discussion

The eight-category FM outline showed no statistically significant association with sex or age group. However, sparse cells, limited power, and wide association-effect CIs do not exclude potentially relevant differences. The hexagonal category was most frequent (24%), as in a Saudi CT series [12]; other studies have reported more oval outlines [3,13]. The exploratory three-category analysis suggested a greater proportion of polygonal outlines in the older group ($p = 0.038$). However, the regrouping was not prespecified, the finding was not multiplicity-adjusted, and its clinical relevance is uncertain. Differences among studies may reflect observer judgment, the imaging plane, and classification scheme [3,12,14].

Measurement reliability and axial-plane limitations

The matched 20-case subsample showed strong intraobserver and interobserver agreement for AP and TD and substantial-to-high categorical agreement for shape. These estimates reflect the designated 20-scan subsample and may not fully characterize measurement variability in the complete cohort. They do not rule out systematic landmark error shared by observers using the same native axial section. Differences in a few shape classifications (two intraobserver and four interobserver disagreements) also demonstrate that the eight-category rubric remains partly subjective. The source-DICOM review of participant 27 addresses the unusual individual observation, but systematic FM-aligned multiplanar remeasurement across the cohort would be needed to assess possible axial-plane bias.

Sex differences in FM dimensions

AP diameter, TD, and estimated area were greater in men, with Cohen's d-values of 0.73-0.97. This direction agrees with CT/CBCT findings from coastal Karnataka [11], Türkiye [3,10], Peru [16], Tibet [17], and Nepal [18], although absolute values vary by population and method. Dry-skull and MRI measurements are not directly interchangeable with axial CT [1,14,17]. Standardized head positioning and 0° gantry tilt reduce between-scan variation in the present series, but an axial section chosen at the apparent widest aperture may still underestimate a true midsagittal basion-opisthion distance. Without multiplanar verification, systematic plane-dependent bias cannot be quantified. Body and skull dimensions were unavailable;

therefore, the sex differences could not be adjusted for overall skeletal size.

The estimated area produced the largest t statistic among the four variables, consistent with reports that estimated FM area can aid sex discrimination [10]. In the Turkish CT study by Meral et al., area performed best among the tested FM measurements, with 75% classification accuracy [10]; this external result should not be attributed to the present sample. The area here was calculated using an elliptical approximation rather than direct segmentation of the outline; therefore, it is a reproducible estimate derived from two perpendicular distances, not the traced bony area. Moreover, group-level significance does not establish individual classification accuracy: no discriminant function, receiver operating characteristic curve, or validation model was evaluated.

The FM index, a proportional rather than absolute measure, did not differ significantly between men and women, as reported in Turkish and Tibetan populations [1,3,17]. Bahşi et al. likewise found significant sex differences in linear dimensions and area without a significant difference in the index [3]. Because the index divides width by length, it describes relative configuration but can obscure an overall size difference when both measurements change together. Golden-ratio studies illustrate continuing interest in proportional FM descriptors [19,20], but their usefulness for individual sex estimation remains uncertain.

No age-related association was detected in the two-group comparisons or in sex-adjusted continuous-age models. This agrees in direction with some adult reports [3,14,17], but CIs permit modest differences, and the study was not designed to test equivalence or adequately assess age × sex interaction. As a cross-sectional study of adults aged 18-55 years, it cannot establish that an individual's FM dimensions are unchanged across adulthood. Pediatric imaging investigations address a different developmental age range and cannot be used to infer longitudinal changes in this adult cohort [21,22].

Forensic and clinical implications

Forensic applications should remain adjunctive: systematic reviews report variable, generally moderate classification performance across populations [8,9], and studies from India, Nepal, Jordan, and Türkiye show that discrimination accuracy depends on the measurements selected and the study setting [11,18,23,24]. The present findings are descriptive measurements from one center, rather than evidence that sex can be determined reliably from FM dimensions alone.

Clinically, local morphometric data may help orientation at the craniovertebral junction, although surgical decisions also depend on the occipital condyles and adjacent neurovascular structures [2,25]. An ovoid FM, defined under its authors' own classification, has been associated with more complications in anterolateral FM meningioma surgery [4], and these tumors have also been classified by their position relative to the neurovascular bundle [5]. FM dimensions remain relevant to Chiari I deformity and achondroplasia-associated stenosis [6,7]. Population means should never dictate surgical margins or osteotomy limits in an individual patient: in this sample, the AP diameter ranged from 28.20 to 41.30 mm and TD from 23.50 to 36.00 mm. Treatment planning requires the patient's own CT or MRI and clinical findings, and the present values should not be used as diagnostic cut-offs.

Limitations

This single-center study enrolled an intentionally sex-balanced quota sample of clinically referred patients, rather than a representative sample of Gujarat or western India. The departmental screening log and radiology acquisition records were checked against the reported recruitment figures and CT protocol; however, the sampling design limits generalizability. Ethnicity or community, body size, and head size were not recorded. Reliability estimates were based on a designated 20-participant subsample; their generalizability beyond this subset is uncertain, and the observation dates and original reading documentation should be retained for audit. Shape grading remained partly subjective, with two intraobserver and four interobserver disagreements. Native axial measurements, without FM-aligned multiplanar validation, may share systematic plane bias despite high ICCs. Participant 27 had a wider-than-long FM, confirmed by repeated measurements and independent source-DICOM review without an identified osseous abnormality; the cross-sectional CT method cannot exclude all systematic plane-related measurement error. No a priori sample-size calculation was performed, and sparse shape categories and modest age effects were assessed imprecisely. The descriptive sex differences are not a validated individual-level prediction model.

Conclusions

In this single-center CT series of 100 adults, AP diameter, TD, and estimated FM area were greater in men. No statistically significant differences in FM shape or index by sex or in the measured parameters by age were detected; however, limited precision precludes conclusions of equivalence. Repeat measurements in a 20-scan subsample showed strong observer agreement, and the unusual wider-than-long foramen was independently confirmed by DICOM review. The native axial imaging plane and the clinical sampling frame remain limitations. These descriptive findings do not establish a validated method for forensic sex classification.

Additional Information

Author Contributions

All authors have reviewed the final version to be published and agreed to be accountable for all aspects of the work.

Concept and design: Bhavesh Kumar, Shivani Chawla

Acquisition, analysis, or interpretation of data: Bhavesh Kumar, Kantilal M. Parmar

Drafting of the manuscript: Bhavesh Kumar, Shivani Chawla

Critical review of the manuscript for important intellectual content: Bhavesh Kumar, Kantilal M. Parmar

Supervision: Kantilal M. Parmar, Shivani Chawla

Disclosures

Human subjects: Informed consent for treatment and open access publication was obtained or waived by all participants in this study. Parul University issued approval PUIECHR/PIMSR/00/081734/8207. The Institutional Ethics Committee on Human Research of Parul University has reviewed, discussed, and approved your proposal titled “Morphometric and Radiomorphometric Analysis of Various Structures Present in the Cranial Fossae of the Human Skull,” which was presented to the committee at its 82nd meeting held on December 31, 2024. **Animal subjects:** All authors have confirmed that this study did not involve animal subjects or tissue. **Conflicts of interest:** In compliance with the ICMJE uniform disclosure form, all authors declare the following: **Payment/services info:** All authors have declared that no financial support was received from any organization for the submitted work. **Financial relationships:** All authors have declared that they have no financial relationships at present or within the previous three years with any organizations that might have an interest in the submitted work. **Other relationships:** All authors have declared that there are no other relationships or activities that could appear to have influenced the submitted work.

References

1. Demir BT, Eşme S, Patat D, Bilecenoğlu B: Clinical and anatomical importance of foramen magnum and craniocervical junction structures in the perspective of surgical approaches. Anat Cell Biol. 2023, 56:342-9. 10.5115/acb.23.006
2. Thintharua P, Chentanez V: Morphological analysis and morphometry of the occipital condyle and its relationship to the foramen magnum, jugular foramen, and hypoglossal canal: implications for craniovertebral junction surgery. Anat Cell Biol. 2023, 56:61-8. 10.5115/acb.22.105
3. Bahşi İ, Adanır SS, Orhan M, Kervancıoğlu P, Büyükbeşe ZS, Beger O, Yalçın ED: Anatomical evaluation of the foramen magnum on cone-beam computed tomography images and review of literature. Cureus. 2021, 13:e19385. 10.7759/cureus.19385
4. Kina H, Erginoglu U, Hanalioglu S, Ozaydin B, Baskaya MK: Ovoid foramen magnum shape is associated with increased complications and decreased extent of resection for anterolateral foramen magnum meningiomas. J Neurol Surg B Skull Base. 2021, 82:682-8. 10.1055/s-0040-1715559
5. Gattozzi DA, Erginoglu U, Khanna O, Hosokawa PW, Martinez-Perez R, Baskaya MK, Youssef AS: Novel classification of foramen magnum meningiomas predicted by topographic position relative to neurovascular bundle. Acta Neurochir (Wien). 2024, 166:199. 10.1007/s00701-024-06091-1
6. Loftus JR, Wassef C, Ellika S: Chiari I deformity: beyond 5 mm below the foramen magnum . Radiographics. 2024, 44:e230227. 10.1148/rg.230227
7. Zhang CH, D'Arco F, Borghi A, Picariello S, Cheung M, Irving M, Thompson D: Unravelling the pathogenesis of foramen magnum stenosis in patients with severe achondroplasia: a CT-based comparison with age-matched controls and FGFR3 craniosynostosis syndromes. Childs Nerv Syst. 2023, 39:3491-9. 10.1007/s00381-023-06005-z
8. Fernandes AL, Shetti A, Lagali-Jirge V, Keluskar V: Accuracy of sex estimation by morphometric evaluation of foramen magnum using computed tomography - a systematic review and meta-analysis. Forensic Sci Med Pathol. 2024, 20:268-79. 10.1007/s12024-023-00613-6
9. Tsiouris C, Triantafyllou G, Karangeli N, et al.: Morphometric assessment of occipital condyles and foramen magnum reveals enhanced sexual dimorphism detection via 3D imaging: a systematic review and meta-analysis utilizing classification and regression trees. Diagnostics (Basel). 2025, 15:1359. 10.3390/diagnostics15111359
10. Meral O, Toklu BB, Meydan R, Kaya A, Karadayı B, Acar T: Sex estimation from foramen magnum parameters in adult Turkish population: a computed tomography study. Leg Med (Tokyo). 2020, 47:101775. 10.1016/j.legalmed.2020.101775
11. Ahmed J, Namrata, Sujir N, Shenoy N, Archana M, Natarajan S: Evaluation of foramen magnum for sex determination among the population of Dakshina Kannada district: a retrospective CBCT study. ScientificWorldJournal. 2024, 2024:6825489. 10.1155/2024/6825489
12. Aljarrah K, Packirisamy V, Al Anazi N, Nayak SB: Morphometric analysis of foramen magnum and occipital condyle using CT images for sex determination in a Saudi Arabian population. Morphologie. 2022, 106:260-

70. 10.1016/j.morpho.2021.07.006
13. Hendricks S, Ishwarkumar S, Pillay P: A morphometric and morphological analysis of the foramen magnum, hypoglossal canal and occipital condyles in a select South African population. Folia Morphol (Warsz). 2024, 83:412-6. 10.5603/fm.95734
14. Gawlikowska-Sroka AK, Gromnicka D, Szczurowski J, Moryś J, Dzięcioł-Anikiej Z, Dzięciołowska-Baran E: Morphometric variability of the foramen magnum in a historical skeletal series from Rome (17th-19th century): limited sexual dimorphism and age-related stability. Folia Morphol (Warsz). 2026, 85:e01726136. 10.5603/fm.112244
15. Verma P, Tiwari P, Hefner JT, et al.: Sex estimation using craniometric data obtained through computed tomography with a sample from Gujarat, India. Forensic Anthropol. 2026, 9:97-105. 10.5744/fa.2025.0011
16. Yataco-Wilcas CA, Salazar-Ascurra A, Diaz-Llanes BE, Coasaca-Tito YS, Lengua-Vega LA, Salazar-Campos CE: Morphometric analysis of the foramen magnum in the Peruvian population . Surg Neurol Int. 2024, 15:9. 10.25259/SNI_936_2023
17. Wang X, Wang Z, Su M, Zhong H: MRI-based foramen magnum morphometry in tibetan adults: sexual dimorphism and findings across adult age groups [IN PRESS]. J Craniofac Surg. 2026, 10.1097/SCS.0000000000012597
18. Atreya A, Shrestha R, Bhandari K, Malla SK, Acharya S, Menezes RG: Morphometric analysis of the foramen magnum in sex estimation: an additional 3DCT study from Nepal on a larger sample. Health Sci Rep. 2023, 6:e999. 10.1002/hsr2.999
19. Ulcay T, Kamaşak B, Görgülü Ö, Uzun A, Aycan K: A golden ratio for foramen magnum: an anatomical pilot study. Folia Morphol (Warsz). 2022, 81:220-6. 10.5603/FM.a2021.0018
20. Dulkadir R, Ulcay T, Görgülü Ö, et al.: A new golden ratio for foramen magnum in pre- and post-adolescent children. Sci Rep. 2025, 15:24495. 10.1038/s41598-025-10505-0
21. Wilk R, Moroz M, Zięba K, Likus W: Foramen magnum morphometry in children based on computed tomography examination. Folia Morphol (Warsz). 2023, 82:587-95. 10.5603/FM.a2022.0066
22. Hamdan SNSM, Rahmat RA, Ibrahim N: Sex estimation of the foramen magnum using computed tomography data in Malaysian juveniles. Med Sci Law. 2026, 66:245-53. 10.1177/00258024251380960
23. Kalbouneh H, Mubarak N, Shwaqfeh J, et al.: Estimation of sex from measurements of foramen magnum region in a contemporary Jordanian population: a computed tomographic study. Anthropol Anz. 2021, 78:317-29. 10.1127/anthranz/2021/1460
24. Kartal E, Etli Y, Asirdizer M, et al.: Sex estimation using foramen magnum measurements, discriminant analyses and artificial neural networks on an eastern Turkish population sample. Leg Med (Tokyo). 2022, 59:102143. 10.1016/j.legalmed.2022.102143
25. Evli C, Kolsuz ME, Orhan K: Retrospective evaluation of the morpometric and morphological anatomy of the occipital condyle, hypoglossal canal and foramen magnum in Turkish populaton with CBCT. Surg Radiol Anat. 2023, 45:795-805. 10.1007/s00276-023-03153-4